Title

Widespread neural reorganization related to expertise in reading visual Braille

Contributors

Cerpelloni F.[1,2], Van Audenhaege A.[1], Matuszewski J.[1], Gau R.[1], Battal C.[1], Falagiarda F.[1], Op de Beeck H.[2*], Collignon O.[1,3*]

Affiliations

(1) Institute of Psychology (IPSY) & Institute of Neuroscience (IoNS), UCLouvain, Belgium

(2) Department of Brain and Cognition, Leuven Brain Institute, KU Leuven, Belgium

(3) HES-SO Valais-Wallis, The Sense Innovation and Research Center, Lausanne & Sion, Switzerland

Corresponding Authors

Filippo Cerpelloni: filippo.cerpelloni@uclouvain.be

Hans Op de Beeck: hans.opdebeeck@kuleuven.be

Olivier Collignon: olivier.collignon@uclouvain.be

* These authors share last authorship

Abstract

Shape features are crucial for reading. Here we investigate the effect of expertise in reading visual Braille, a script developed for touch that does not share the typical explicit shape information of other alphabets. We compared visual Braille readers and a naïve control group and found that individually localized visual word form area VWFA) was selectively activated for visual Braille when compared to scrambled Braille, but only in expert Braille readers. Multivariate analyses showed that linguistic properties can be decoded from Latin in both groups and from Braille in expert readers. Yet, cross-script generalization failed to reveal common representations across Latin and Braille scripts in experts, suggesting script-specific orthographic representations. Primary visual cortex, shape-selective areas (LO), and linguistic areas (l-PosTemp) showed similar multivariate profiles to VWFA, but with cross-script generalization in left Posterior Temporal area only. We conclude that the linguistic properties of a visual script, rather than low-level line-junctions properties, play a major role in how the visual system, and VWFA in particular, processes scripts.

Introduction

Object recognition is a paramount process for most species to understand and navigate their surroundings (Logothetis & Sheinberg, 1996). In vision, object recognition is modelled as a hierarchical process going from the detection of simple features to their progressive integration in more complex shapes (Riesenhuber & Poggio, 1999; Marr & Hildreth, 1980; Biederman, 1987; Krizhevsky et al., 2017). Texture and colour (Witzel & Gegenfurtner, 2018; Bramão et al., 2011) also contribute to human object recognition, but not to the same extent as shape (Biederman, 1987; Grill-Spector & Malach, 2004; Landau et al., 1988; Tarr & Bulthoff, 1998). Shape is generally conceived as an arrangement formed by lines joined together in a particular way, or by lines around the outer edge of an object (*Definition of Shape*). The flexibility of shape processing in the human brain has allowed the development of written scripts and highly complex visual stimuli with symbolic meaning. Most written systems developed throughout history share basic shape features with natural objects (Changizi et al., 2006). Core features of visual object recognition may have been co-opted for written word recognition (Dehaene et al., 2005), exerting pressure for scripts to appear the way they do. Supporting this idea, the basic sensitivity to symbols from a script seems to be present in untrained monkeys (Rajalingham et al., 2020), further illustrating how culturally invented scripts may have been optimized from the natural scaffolding of shape processing in the brains of primates.

In the human brain, visual scripts more specifically activate a region referred to as the visual word form area (VWFA) (Cohen et al., 2000, 2002). This region is a primary example of brain adaptation to a cultural invention, as this region only emerges if and when humans learn to read (Dehaene et al., 2010, 2015; Dehaene & Cohen, 2011; Dehaene-Lambertz et al., 2018). The presence of pre-existing shape selectivity in VWFA is one of the most often mentioned causes of the location of this region (Dehaene & Cohen, 2011; Dehaene-Lambertz et al., 2018). Several studies support the crucial role of shape in the word form system: the importance of line junctions for fluent reading (Bola et al., 2017), the partial overlap between VWFA and the areas of the ventral visual cortex that respond selectively to line junctions (Szwed et al., 2011), an equal response to line drawings of objects and false fonts (Ben-Shachar et al., 2007), and comparable levels of activation for both known letters and foreign characters (Vogel et al., 2012; Xue & Poldrack, 2007). All these results led to the suggestion that instead of responding specifically to visual words, VWFA, along with other regions located in the fusiform gyrus, might be involved in complex shape processing more generally (Li et al., 2024; Roberts et al., 2013). An alternative account of VWFA downplays the role of visual

features and emphasizes the integration of this visual region with downstream language regions involved in phonological and semantic processing (Price & Devlin, 2003, 2004, 2011). Structural and functional connectivity between VWFA and the traditional language network, even before infants learn to read (Saygin et al., 2016; Li et al., 2020; Stevens et al., 2017), support the interactive account of VWFA. Evidence from tactile Braille reading, both in visually impaired (Büchel et al., 1998; Price & Devlin, 2003) and sighted individuals (Siuda-Krzywicka et al., 2016), and activations for speech processing (Pattamadilok et al., 2019; Planton et al., 2019, 2022; Wang et al., 2022) further support the idea that VWFA processes linguistic information more generally, rather than being a purely visual area.

To disentangle the role of shape-based processing and nonvisual accounts for how the visual system adapts to reading new scripts, one needs to compare word form selectivity for shape-based scripts with selectivity for a script that lacks classical shapes features and line junctions. This situation is provided by visual Braille. Visually, Braille is not optimal, since it possesses no shape cues like lines, junctions, and clear outer shapes that are thought as necessary for efficient reading (Bola et al., 2017). However, rare visual Braille experts, involved usually in professional teaching of tactile Braille to blind individuals, can read Braille by visually processing the dot patterns that compose words. Thus, in reading Braille visually, stimuli engage the same sense, and possess the same linguistic content as the native alphabet; but vary widely in terms of visual features. The study of people who learn to read Braille visually therefore allows one to trace how the reading network, accustomed to typical (visual) input, is co-opted by atypical orthographic material composed of dots.

Here we present two fMRI experiments that investigate how the visual system adapts to learning a shapeless script by comparing brain activity of people experts in visual Braille with non-experts, testing both visual Braille and the native shape-based script for these populations (Latin-based French). First, we tested whether the word form system activated for a Latin script is activated by reading visual Braille (figure 1A). Second, we tested whether the same coding principles are used for the Braille script in terms of relationships between stimuli with different linguistic properties. Building on previous work for shape-based scripts (Szwed et al., 2014), we further explored whether other regions involved in reading, including early visual cortex (V1), shape-selective regions (Lateral Occipital, LO), and linguistic region in posterior temporal areas, show similar changes as to the ones hypothesised for VWFA. Overall, we show that expert visual Braille readers show overwhelming similarities between brain regions processing Latin and Braille scripts, showing the flexibility of the reading network for processing scripts even when made of atypical visual features like Braille.

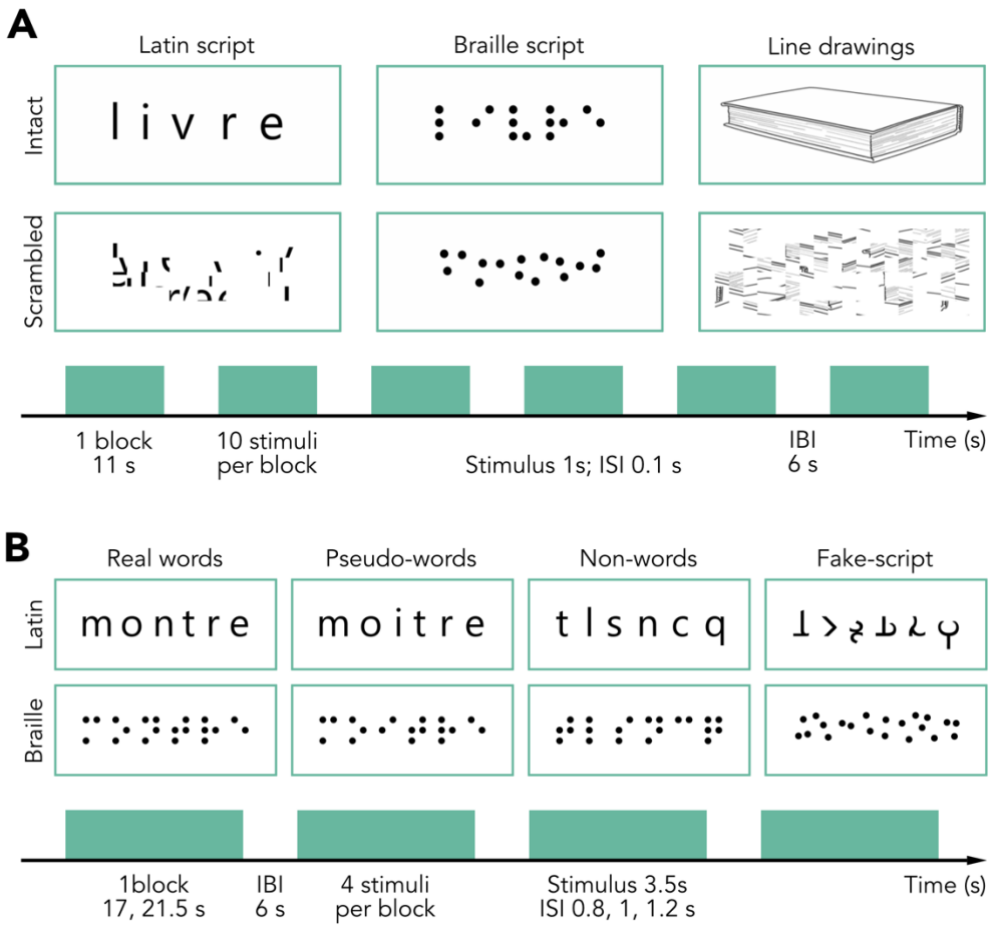

Figure 1 – Experimental design and examples of stimuli for experiments 1 and 2. **(A)** Experiment 1: functional localizer. We presented six categories of stimuli (intact and scrambled Latin-script words, Braille words and line drawings) to participants in an fMRI block design. Each participant underwent two runs in which six blocks for each category were presented in pseudo-randomized order. Blocks lasted for 11 seconds and were separated by a fixed inter-block interval (IBI) of 6 seconds. Each block consisted of ten stimuli from one category, each for a duration of 1 second and with an inter-stimulus interval (ISI) of 0.1s. During the session, participants performed a 1-back task to detect the repetition of a stimulus. The target was present in 10% of the blocks. **(B)** Experiment 2: Coding of linguistic properties. Four different linguistic conditions (Real Words, Pseudo-Words, Non-Words, Fake Script) for each script (Latin, Braille) were used. We presented these categories of stimuli (intact and scrambled Latin-script words, Braille words, line drawings) to participants in a fMRI block design. Each participant underwent twelve sessions in total, six for each script (counterbalanced across subjects). In each run, three blocks for each category of one script were presented in a pseudo-randomized order. Each block lasted for 17 or 21.5 seconds, depending on the presence of a target, with a 6-second IBI separating the two blocks. Four 4 stimuli from the same category were presented within a block, each for 3.5 seconds, with a jittered ISI of 0.8, 1, or 1.2 seconds. During the session, participants performed a 1-back task to detect the repetition of a stimulus. The target was present in 10% of the blocks. The position of the target, as well as jittered ISI, block order, and stimuli order, were counterbalanced across runs.

Results

The Visual Word Form Area of expert readers is selective to visual Braille

The first major question in our study was whether the VWFA as activated by the Latin script is also activated by visual Braille in experts. In all eighteen subjects that took part in the experiment and showed a VWFA for the Latin script (six expert Braille readers, twelve control

participants), we performed a Generalised Linear Model (GLM) and contrasted univariate activations for intact over scrambled Latin script words (FW > SFW) and for intact over scrambled Braille words (BW > SBW). In the expert group, individual clusters appeared in the [BW > SBW] contrast, in similar sites to the response to Latin-based stimuli (Figure 2). We performed Small Volume Correction at an individual level by drawing a 10mm radius sphere in the [BW > SBW] contrast around the peak coordinates in VWFA separately and individually identified through the [FW > SFW] contrast. A significant selective response for Braille (BW > SBW) in 5 of the 6 experts emerged in VWFA defined from Latin-based French (Table 1). In the control group, only 1 out of 12 subjects showed a small significant cluster (Table S1, Supplementary Material). The proportion of activations in participants was significantly different between the two groups (Chi-square = 7.03, $p = 0.008$), showing that people who can read Braille through the visual modality activate VWFA, regardless of the lack of visual features present in canonical scripts (Changizi et al., 2006). We additionally estimated Dice coefficients, a measure of overlap as intersection of two areas divided by the sum of the voxels in the individual areas, individually for each expert. Where VWFA activation for both scripts was present ($p_{uncorr} < 0.001$), we found an overlap between scripts of 34% on average (range 8 - 53%). Next, we investigated whether a significant preference for intact over scrambled Braille was also present in our expert group as a whole (Figure S1, Supplementary Material), through paired t-tests on the mean activation for intact or scrambled Braille stimuli. We found a significant difference between intact and scrambled Braille in VWFA defined through the Latin-based script ($t_{(5)} = 4.45$, $p = 0.006$). This finding was not influenced by including regressors controlling for eye movements through a decoding of eye motion from fMRI time series using bidsMReye (Gau & Cabee, 2023) and deepMReye (Frey et al., 2021). This finding is in line with the aforementioned observation of significant clusters of Braille selectivity in/near Latin-based VWFA.

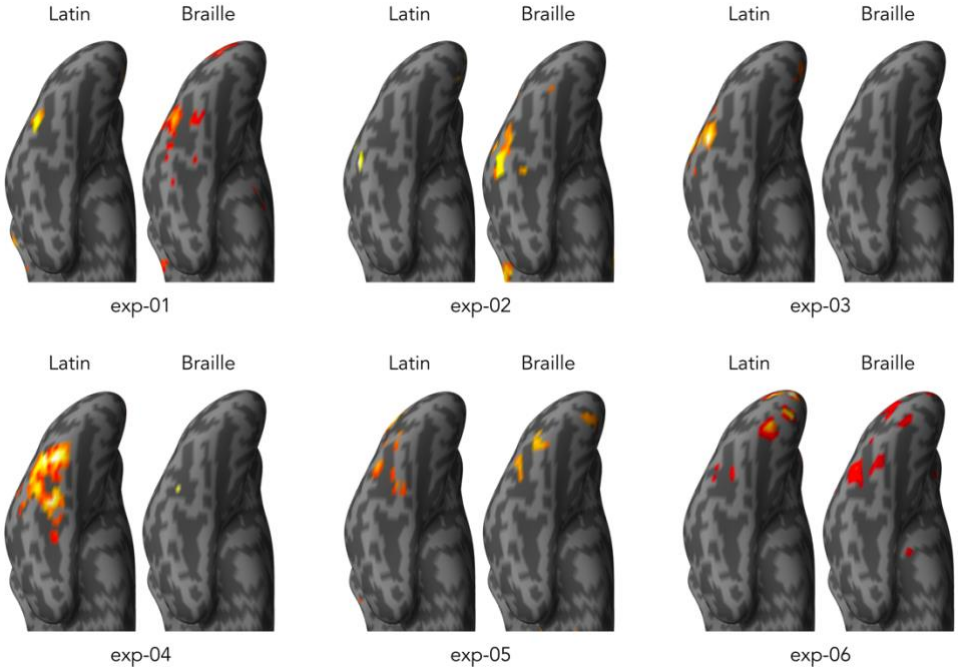

Figure 2 – Visual Word Form Area's univariate response to visual Braille in experts. Results of each expert participant for [FW > SFW] and [BW > SBW] contrasts. For each expert visual Braille reader, contrasts for intact over scrambled Latin stimuli (left side of each participant) and intact over scrambled Braille stimuli (right side of each participant). All results are p_{uncorr} = 0.001 for visualization purposes. Through Small Volume Correction, we identified significant activation for intact over scrambled Braille in sites that localize intact over scrambled Latin stimuli in 5 experts (all except exp-03).

Contrast	Subject	p-value (FWE corrected)	z-score	Cluster size	MNI coordinates
FW > SFW	exp-01	0.000	5.04	24	-47 -60 -13
	exp-02	0.000	4.78	9	-52 -47 -18
	exp-03	0.000	6.57	83	-52 -55 -18
	exp-04	0.000	5.90	159	-44 -63 -13
	exp-05	0.002	4.31	29	-44 -60 -15
	exp-06	0.000	5.27	27	-44 -60 -13
BW > SBW	exp-01	0.000	5.09	113	-49 -63 -13
	exp-02	0.000	5.23	92	-55 -47 -21
	exp-03	NA	NA	NA	NA
	exp-04	0.034	3.50	7	-39 -60 -5
	exp-05	0.003	4.23	37	-42 -57 -8
	exp-06	0.000	5.39	79	-47 -63 -15

Table 1 – Functional activation of Visual Word Form Area (VWFA) in expert visual Braille readers. For each expert, we contrasted intact Latin words (FW) to scrambled ones (SFW) and obtained activation peaks. To determine the cluster size of VWFA, we performed Small Volume Correction in a 10mm radius sphere around the individual peak coordinates of VWFA identified through a Latin-script contrast (FW > SFW). Next, we performed an additional Small Volume Correction around the same peaks to determine significantly activated voxels for the contrast of Braille words (BW) over scrambled dots (SBW). MNI coordinates refer to the peak of each contrast.

Linguistic conditions can be decoded in VWFA when a script is known, regardless of its visual features

To investigate whether the multivariate profiles of VWFA organization was based on linguistic content, we trained a support vector machine (SVM) to classify pairs of conditions in Experiment 2. These conditions (Real Words, Pseudo-Words, Non-Words, Fake Script) differed in the number of linguistic properties presented (see “Methods” section). We decoded pairwise comparisons of linguistic conditions within each script, on an individual level in regions defined by selectivity for intact over scrambled Latin words (Figure 3A). In all the script-group pairs where the stimuli come from a known script (experts seeing Latin-based stimuli, experts seeing Braille stimuli, controls seeing Latin-based stimuli), pairwise decoding accuracy (DA) was on average strongly above chance level (Latin script, expert group: DA = 0.72, $t_{(5)} = 5.850$, $p_{FDR} = 0.002$, D = 2.3; Braille script, expert group: DA = 0.67, $t_{(5)} = 8.386$, $p_{FDR} < 0.001$, D = 3.4; Latin script, control group: DA = 0.72, $t_{(11)} = 5.347$, $p_{FDR} < 0.001$, D = 1.6). In striking contrast, visual Braille decoding in VWFA was not significant in the control group decoding (DA = 0.51, $t_{(11)} = 0.61$, $p_{FDR} = 0.36$).

Additionally, we performed two-tailed t-tests on the decoding accuracies (in case of comparisons within a group, we performed paired t-tests) and found significant differences between known and unknown scripts (Latin, experts – Braille, controls: $t_{(8.6)} = 4.73$, $p_{FDR} = 0.002$, D = 2.5; Braille, experts – Braille, controls: $t_{(12.1)} = 5.95$, $p_{FDR} < 0.001$, D = 2.7; Latin, controls – Braille, controls: $t_{(11)} = 4.88$, $p_{FDR} = 0.0012$, D = 1.7, Figure 3A). In contrast, there were no significant differences between conditions across known scripts ($p_{FDR} > 0.36$). These results suggest that the VWFA of experts encodes the differences between linguistic properties in visual Braille as they do, and as controls do, in their native Latin script, while no such representation is detected for visual Braille in control participants.

Linguistic regularities in VWFA are organized similarly across scripts

Next, we investigated gradients of script-specific representations. We looked in detail at the same pairwise comparisons described in the section above to explore the different relationships between linguistic conditions. We performed within script repeated measures ANOVAs to identify group effects (differences between expert and naïve subjects), effects of the differences in linguistic properties (differences between decoding pairs), and interactions between those two variables (influence of the expertise on the task). In the case of the Braille script, we found an effect of group ($F_{(1)} = 30.825$, $p < 0.001$, $\eta^2_p = 0.66$), as well as an effect of linguistic properties ($F_{(5)} = 6.093$, $p < 0.001$, $\eta^2_p = 0.25$) and an interaction between the two factors ($F_{(5)} = 3.195$, $p = 0.011$, $\eta^2_p = 0.14$), as shown in Figure 3B. These results indicate that the two groups process Braille differently. While VWFA can identify differences between

conditions in the case of expert readers, this is not possible in the control group. In contrast, the analysis of the Latin script only showed an effect of the linguistic properties ($F_{(5)} = 11.240$, $p < 0.001$, $\eta^2_p = 0.4$), but no difference between groups ($F_{(1)} = 0.888$, $p = 0.36$) and no interaction ($F_{(5)} = 0.863$, $p = 0.51$). Post-hoc t-tests on the conditions showed that the classification of Real Words against Pseudo-Words (RW-PW) is different (less accurate) from all the other pairs, except the pseudo- and -non-words pair (RW-NW: $p_{Bonf} = 1$, all other $p_{Bonf} < 0.024$). A full table of the post-hoc results is available in the Supplemental Material (Table S2). Differences between conditions show a sensitivity to the linguistic properties of a script such as enhanced linguistic distances triggers enhanced decoding accuracy for all known scripts (but not for Braille in non-experts). The lack of group differences for the Latin script shows that this sensitivity is induced by differences in expertise in a given script. When groups are compared on their native script (levelling the effect of training), no differences are found.

To compare the organizational patterns between scripts and groups, we performed Representational Similarity Analysis (RSA). We built dissimilarity matrices using the pairwise decoding accuracies of each script-group pair (Figure 3C), as well as for a model of linguistic distance that captures the number of linguistic properties that are different between two conditions (with Real Words and Fake Script being most different). We computed the Pearson's correlations between the values in these dissimilarity matrices, and determined their significance through non-parametric permutation analyses (Mattioni et al., 2020; Stelzer et al., 2013) (see "Methods"). We found high correlations for known scripts, both between patterns of neural activity (Latin, experts – Latin, controls: $r = 0.58$, $p_{FDR} < 0.001$; Braille, experts – Latin, controls: $r = 0.58$ $p_{FDR} < 0.001$) and with the linguistic model (Latin, experts – Model: $r = 0.43$, $p_{FDR} = 0.005$; Braille, experts – Model: $r = 0.59$, $p_{FDR} < 0.0001$; Latin, controls – Model: $r = 0.45$, $p_{FDR} < 0.0001$). Correlations with the dissimilarity matrix for Braille in the control group were mostly absent (all $p_{FDR} > 0.20$), with the exception of a correlation with the matrix for Braille stimuli in expert readers ($r = 0.33$, $p_{FDR} = 0.002$). Overall, these correlations further support the view that Braille script in experts is represented in the VWFA in a similar way as Latin-based stimuli and that the type of representation is related to a theoretical model of overlapping linguistic properties inspired by previous findings (Vinckier et al., 2007).

Linguistic representations in VWFA are not generalized across scripts

Since linguistic conditions in Braille readers could be decoded in both scripts (Braille, Latin) we looked at possible generalizations between scripts. We performed cross-script decoding to see if the SVM classifier trained to distinguish linguistic conditions in one script would be able to decode similar conditions in the other script (Figure 3D). A significant result would indicate that the neural patterns associated with the different conditions partially abstract from the visual features intrinsic to each script and would represent linguistic properties

independently of the script. We limited this analysis to the expert group since it was the only group showing significant decoding in each script separately. The average cross-script decoding accuracy was not significantly higher than chance (DA = 0.54, $t_{(5)}$ = 0.58, p_{FDR} = 0.40). This result was maintained in the comparisons of all pairs of linguistic conditions, where no pair of stimuli showed significant cross-script decoding (highest DA value: RW – PW, DA = 0.56, $t_{(5)}$ = 1.62, p_{FDR} = 0.41).

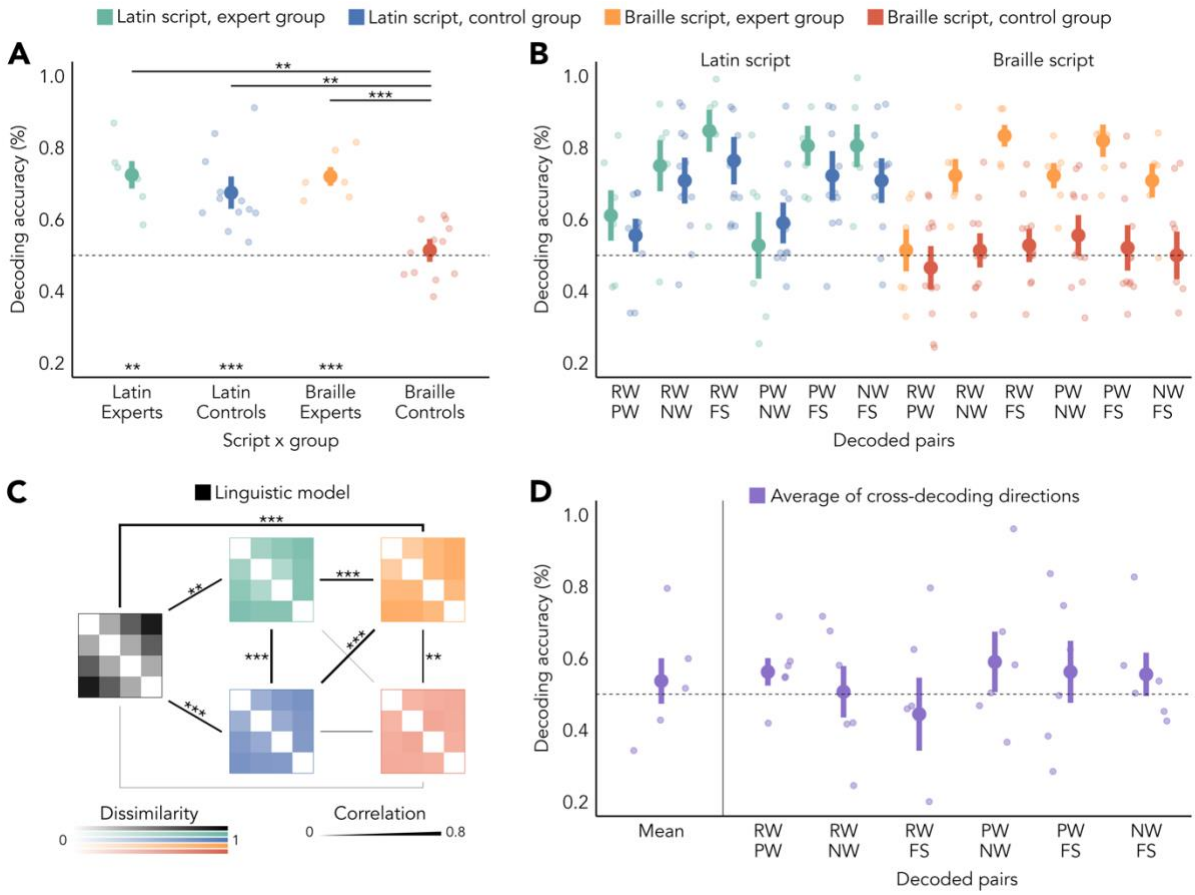

Figure 3 – Multivariate representation of linguistic properties in the Visual Word Form Area (VWFA). **(A)** Average of pairwise decoding of conditions that differ in linguistic properties. In all the known scripts (Latin and Braille in experts, Latin in controls), we found significantly above-chance decoding and significant differences with the unknown and non-decodable condition of Braille presented to a control group. **(B)** Pairwise decoding within scripts. While experts and controls showed no group difference for their common native script, they showed a group difference for Braille, with experts showing a pattern similar to the one of Latin script. **(C)** Representational similarity analysis (RSA) between neural representations (green, orange, blue, red) and with a linguistic model (black). Strength of the correlation is represented by the thickness of the bar connecting two patterns. Organizational patterns of known scripts correlated strongly with each other and with a theoretical model of linguistic distance. A script unknown to the reader (Braille for the control group) does not correlate with the model nor with patterns for Latin script. A significant correlation is present between the neural patterns of Braille. **(D)** Cross-script decoding. The mean of cross-decoding across all pairs of linguistic conditions did not show significant above-chance decoding, and neither did the individual pairs. RW = Real Words; PW = Pseudowords; NW = Nonwords; FS = Fake Script. In all the figures, stars represent significance (* p ≤ 0.05, ** p ≤ 0.01, *** p ≤ 0.001). Error bars represent standard error.

Shape-sensitive Lateral Occipital (LO) does not preferentially process Braille, but represents the differences in linguistic properties

We contrasted fMRI activation for intact and scrambled line drawings to identify individual bilateral Lateral Occipital (LO) sites as two regions of interest (ROIs), one for each hemisphere. To probe for extended plasticity effects of visual Braille in other areas commonly associated with shape, we then performed paired t-tests on the mean activation for intact or scrambled Braille stimuli in those ROIs and found no overall difference in LO (left-LO: $t_{(5)} = 1.50$, $p = 0.19$; right-LO: $t_{(5)} = 1.86$, $p = 0.12$). This result was not dependent on eye movements (figure S2). We then performed the same Multivariate Pattern Analyses applied to VWFA (see "Methods"). In summary, both hemispheres showed similar results as to VWFA. We found significant decoding of linguistic properties (Figures 4A and 4B) only in scripts known by the groups of participants (left-LO: all $p_{FDR} < 0.006$; right-LO: all $p_{FDR} < 0.011$) and not for Braille processed by the control group (all $p_{FDR} > 0.10$). We also observed statistical differences between known scripts and Braille for controls (all $p_{FDR} < 0.031$). In left-LO, we additionally observed differences between Braille in experts and the native script (both $p_{FDR} < 0.033$). Looking within each script, we found effects in line with VWFA. In Braille, we found group differences (both $p \leq 0.002$), but no effects of linguistic properties (both $p \leq 0.11$) nor interactions (both $p > 0.23$). Within Latin, both hemispheres presented a main effect of linguistic properties (both $p < 0.001$), but no group differences (both $p > 0.36$). In left-LO, we found an interaction between groups and linguistic properties (left-LO: $F_{(5)} = 2.959$, $p = 0.018$; right-LO $F_{(5)} = 0.895$, $p = 0.49$). Detailed statistical tests and results are available in tables S3 and S5 in the Supplementary Material. These results indicate that experts' LO represents Braille stimuli, although differently from the way Latin-based stimuli are processed. Representational Similarity Analysis (RSA) on the patterns of pairwise decoding accuracies (Figure 4C) showed strong correlations for known scripts, both between the neural RDMs (left-LO: all $r > 0.55$, all $p_{FDR} < 0.001$. Right-LO: all $r > 0.64$, all $p_{FDR} < 0.001$) and with the linguistic model (all $p_{FDR} \leq 0.002$). In the left-LO of experts, the correlation between Braille-experts RDM with the model was close to significance ($r = 0.34$, $p_{FDR} = 0.052$). Braille representations in controls did not correlate with other neural RDMs or with the model (all $p_{FDR} > 0.07$). No significant cross-script decoding was observed (left-LO: DA = 0.59, $t_{(5)} = 1.56$, $p_{FDR} = 0.16$; right-LO DA = 0.58, $t_{(5)} = 2.35$, $p_{FDR} = 0.10$). Finer comparisons were mostly consistent with a lack of cross-decoding and with what we found in VWFA: except for Real Words contrasted to Pseudo-Words in the left LO (DA = 0.56, $t_{(5)} = 4.39$, $p_{FDR} = 0.025$), we observed no significant cross-decoding being above chance level in each pair-wise instances tested.

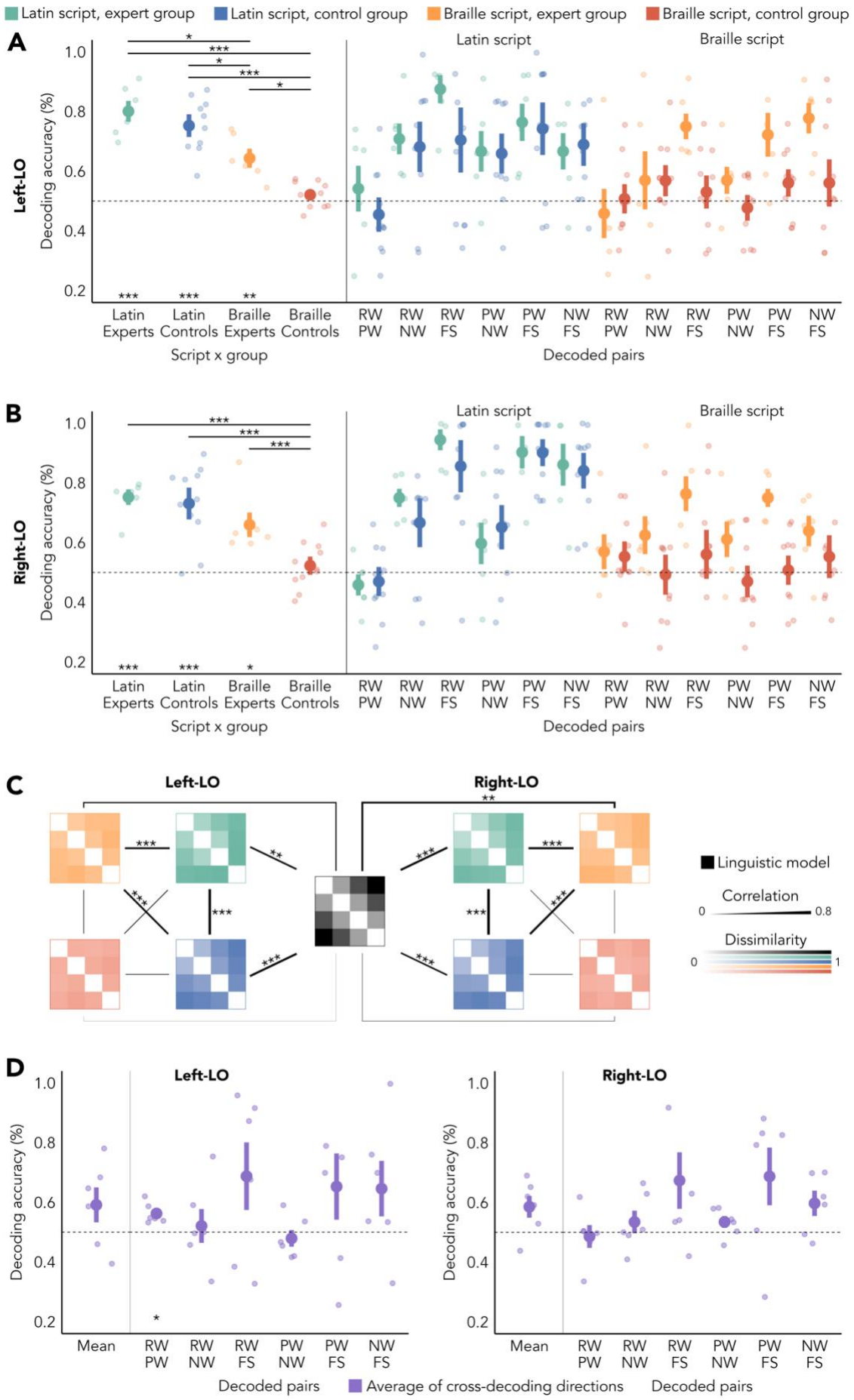
Latin script, expert group
Latin script, control group
Braille script, expert group
Braille script, control group
A
Left-LO
Decoding accuracy (%)
Latin script
Braille script
Latin Experts
Latin Controls
Braille Experts
Braille Controls
Script x group
RW PW
RW NW
RW FS
PW NW
PW FS
NW FS
Decoded pairs
B
Right-LO
C
Left-LO
Right-LO
Linguistic model
Correlation
Dissimilarity
D
Mean
Average of cross-decoding directions

Figure 4 – Multivariate representation of linguistic properties in left and right Lateral Occipital area (LO). **(A)** Pairwise decoding of conditions that differ in linguistic properties in left-LO, average (left) and individual pairs within script (right). Scripts known by the participants showed above-chance decoding accuracy and significant differences with the Braille-experts pair. Significant differences also emerged between the Braille-experts pair and Latin script in both groups. Individual pairs highlighted similar trends within Latin script but different ones within Braille, with experts showing a pattern similar to the one for Latin. **(B)** Pairwise decoding of conditions that differ in linguistic properties in right-LO, average (left) and individual pairs within script (right). Known scripts by the participants showed above-chance decoding accuracy and significant differences with the Braille-experts pair. Individual pairs highlight similar trends within Latin script but different ones within Braille, with experts showing a pattern similar to the one for Latin. **(C)** Representational similarity analysis (RSA) between neural representations (green, orange, blue, red) and with a linguistic model (black). Strength of the correlation is represented by the thickness of the bar connecting two patterns. In left-LO, patterns of known scripts correlate strongly with each other. While Latin script patterns also correlate with the model, ~~Braille~~ representations in experts show an almost-significant trend ($p = 0.052$). In right-LO, only neural RDMs relative to known scripts show correlations between themselves and with the linguistic model. **(D)** Cross-script decoding. The mean of cross-decoding across all pairs of linguistic conditions did not show significant above-chance decoding. In right-LO (right plot), no individual comparison, nor the mean, can be decoded across scripts. RW = Real Words; PW = Pseudowords; NW = Nonwords; FS = Fake Script. In all the figures, stars represent significance (* $p \leq 0.05$, ** $p \leq 0.01$, *** $p \leq 0.001$). Error bars represent standard error.

Multivariate coding of linguistic properties of visual Braille extends to early visual cortex

We further extended our analysis of the organizational pattern found in VWFA and LO, to see if widespread visual Braille processing involves earlier stages of visual perception. To identify the region of interest, we relied on the early visual cortex (V1) mask from Anatomy toolbox (Eickhoff et al., 2005) and overlapped it with an independent contrast to determine overall visual activity as extracted from the Generalised Linear Model (GLM) for each participant (intact and scrambled Latin words over rest, see “Methods”). Paired t-tests on the mean activation for intact or scrambled Braille stimuli showed no overall difference ($t_{(5)} = 3.67$, $p = 0.07$). This result was confirmed also when we controlled for eye movements (figure S2). On the multivariate level (figure 5A), we found above chance decoding for all scripts (all $p_{FDR} <= 0.02$). Moreover, decoding accuracies of known scripts differed from participants seeing an unknown script (all $p_{FDR} < 0.042$). Then, we performed repeated measures ANOVAs for individual scripts. Braille script (Figure 5B) showed a significant main effect of group ($F_{(1)} = 10.611$, $p = 0.005$), and of linguistic differences ($F_{(5)} = 5.818$, $p < 0.001$), as well as an interaction between the two ($F_{(5)} = 3.011$, $p = 0.015$). Only experts showed distinctions in the neural patterns associated with different linguistic properties of the stimuli. Expectedly, Latin script only showed a main effect of the linguistic properties compared ($F_{(5)} = 7.475$, $p < 0.001$), with no differences between groups ($F_{(1)} = 0.007$, $p = 0.94$). Post-hoc tests showed that the difference between real and Pseudo-Words, the classification of stimuli that share the most linguistic features, is significantly different from (lower than) all the other comparisons of conditions (all $p_{Bonf} < 0.004$). These results indicate that, while Latin script is processed similarly in the two groups, a group difference is present in Braille, surely due to the difference of Braille expertise between our participants. Neural pattern of linguistic distances (Figure 5C)

showed significant correlations between the neural RDMs for known scripts (all $p_{FDR} < 0.001$) and between scripts in the control group (Latin, Controls – Braille, Controls, $r = 0.22$, $p_{FDR} = 0.021$), suggesting that the processing of Braille in the expert group is similarly organized to the processing of the Latin script in both groups. The linguistic model correlated significantly with representations of Latin script stimuli (all $p_{FDR} < 0.026$) but, in contrast to the findings in all other ROIs, not with representations for Braille stimuli (all $p_{FDR} > 0.09$). Lastly, we did not find any significant cross-script decoding in V1 (Figure 5D), neither in the average of the comparison pairs (DA: 0.49, $t_{(5)} = -0.36$, $p_{FDR} = 0.86$) nor in the single pairs (most significant value: RW – FS, DA = 0.53, $t_{(5)} = 0.72$, $p_{FDR} = 0.71$), hinting that the distinct low-level visual features of the two scripts result in separate representations. Detailed statistical tests and results are available in table S7 in the Supplementary Material.

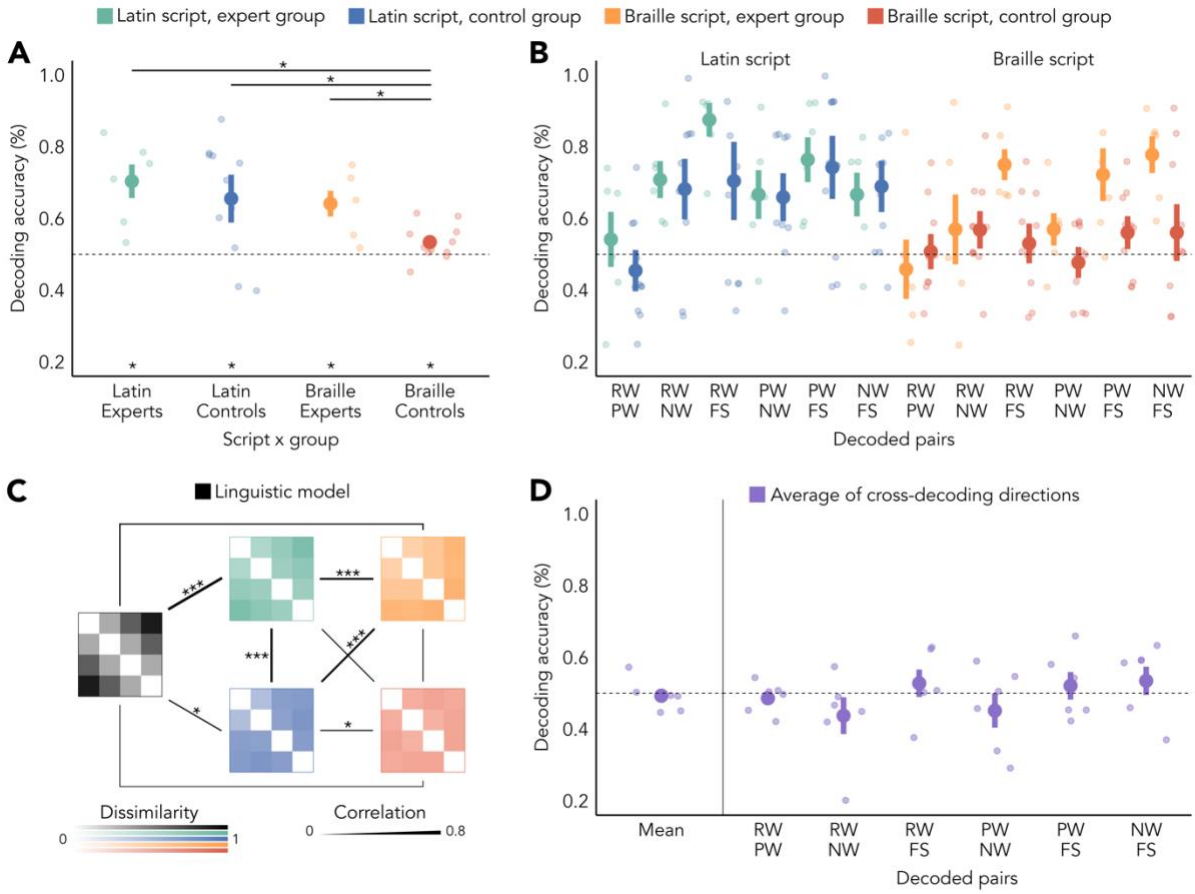

Figure 5 – Multivariate representation of linguistic properties in V1. **(A)** Average of pairwise decoding of conditions that differ in linguistic properties. Stars above the labels on the x-axis represent the statistical significance of the decoding accuracy, while stars above the horizontal bars on top of the graph represent the significance of the difference between conditions (* $p \leq 0.05$, ** $p \leq 0.01$, *** $p \leq 0.001$). Error bars represent standard error. In all the script-group pairs, we found significantly above-chance decoding and significant differences with the unknown and non-decodable condition of Braille presented to a control group. **(B)** Pairwise decoding within scripts. While experts and controls showed no group difference for their common native script, they showed a group difference for Braille, together with a main effect of condition and interaction between the variables, with experts showing a pattern similar to the one of Latin script. **(C)** Representational similarity analysis (RSA) between neural representations (green, orange, blue, red) and with a linguistic model (black). Strength of the correlation is represented by the thickness of the bar connecting two patterns. In V1, patterns of known scripts correlate strongly with each other. Patterns relative to control participants showed a significant correlation across

scripts. Only the neural RDMs relative to the organization of the Latin script show a correlation with the linguistic distance model, contrary to what happens in the case of Braille. **(D)** Cross-script decoding. The mean of cross-decoding across all pairs of linguistic conditions did not show significant above-chance decoding, and neither did the individual pairs. RW = Real Words; PW = Pseudowords; NW = Nonwords; FS = Fake Script.

Script-independent representation of linguistic properties in the Left Posterior Temporal Region

Lastly, we observed reliable activations outside of our ROIs when we contrasted intact Latin words over scrambled ones. By masking these activations to regions of the language network (Fedorenko et al., 2010), we identified the left-posterior temporal region, as a higher-order linguistic area. We limited our analyses to those subjects who show univariate activation for Latin words (fifteen participants, five experts). Paired t-test on the mean activation for intact Braille and scrambled dots did not highlight overall preferential activations by intact Braille in the expert group as a whole ($t_{(4)} = 2.05$, $p = 0.11$), nor in the control group, as expected ($t_{(10)} = -1.24$, $p = 0.24$). These results did not change when eye movements were considered in the GLM. Multivariate analyses within each script revealed an overall profile very similar to the one previously seen in other ROIs. Pairwise comparisons (Figure 6A) could be significantly decoded if the script is known by the participants (all $p_{FDR} < 0.001$), while the script that is unknown to the group had chance-level accuracy (DA = 0.52, $t_{(9)} = 0.925$, $p_{FDR} = 0.24$), and significant differences emerged between scripts known and not known by the group of participants (all $p_{FDR} < 0.001$). More in-depth, pairs of comparison (figure 6B) showed large differences within Braille (group effect: $F_{(1)} = 58.416$, $p < 0.001$; condition effect: $F_{(5)} = 4.229$, $p = 0.002$), while in the Latin script we observed only an effect of conditions ($F_{(5)} = 4.991$, $p = 0.001$) and no group differences ($F_{(1)} = 0.833$, $p = 0.38$). Post-hoc analyses on the differences between the conditions show that shared linguistic properties are harder to decode (RW-PW and PW-NW, $p_{Bonf} = 0.38$) than more linguistically distant comparisons ($p_{Bonf} < 0.017$). The similarity structure of pairwise comparisons (Figure 6C) showed significant correlations between known scripts (all $p_{FDR} < 0.001$) and no correlation with unknown scripts. Intriguingly, no neural RDM correlated with our linguistic model (all $p_{FDR} > 0.06$). The lack of correlation to the theoretical model suggests different coding principles compared to the other ROIs. Even more striking, and in contrast to all other ROIs, we found the average pairwise cross-decoding accuracy (figure 6D) to be significantly higher than chance (DA = 0.66, $t_{(5)} = 4.08$, $p_{FDR} = 0.02$, D = 1.8). More in detail, several of the cross-scripts binary decoding were significant (RW-NW, : DA = 0.78, $t_{(5)} = 4.49$, $p_{FDR} = 0.02$; PW-NW: DA = 0.68, $t_{(5)} = 3.64$, $p_{FDR} = 0.025$; PW-FS: DA = 0.68, $t_{(5)} = 2.69$, $p_{FDR} = 0.038$; NW-FS: DA = 0.75, $t_{(5)} = 3.35$, $p_{FDR} = 0.025$). Real Words compared to the Fake Script did not seem to generalize (DA = 0.52, $t_{(5)} = 0.293$, $p_{FDR} = 0.39$). A borderline-significant trend emerged instead in the generalization of the comparison

between Real Words and Pseudo-Words (DA = 0.58, $t_{(5)} = 2.36$, $p_{FDR} = 0.052$, D = 1). These findings reveal, overall, a script-independent representation of linguistic content. Detailed statistical tests and results are available in table S9 in the Supplementary Material.

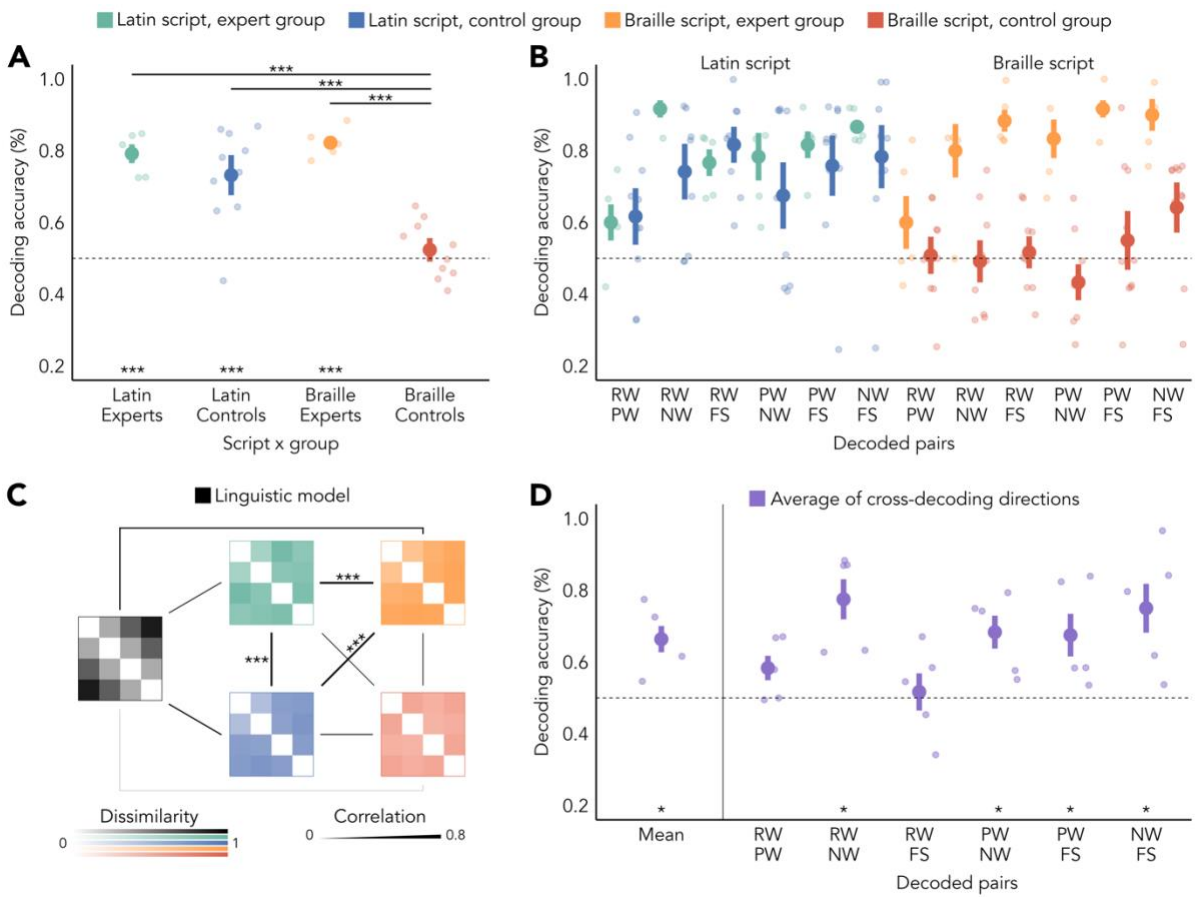

Figure 6 – Multivariate representation of linguistic properties in PosTemp. **(A)** Average of pairwise decoding of conditions that differ in linguistic properties. In all the known scripts (Latin and Braille in experts, Latin in controls), we found significantly above-chance decoding and strong significant differences with the unknown and non-decodable condition of Braille presented to a control group. **(B)** Pairwise decoding within scripts. While experts and controls showed no group difference for their common native script, they showed a group difference for Braille, with experts showing a pattern similar to the one of Latin script. **(C)** Representational similarity analysis (RSA) between neural representations (green, orange, blue, red) and with a linguistic model (black). Strength of correlation is represented by the thickness of the bar connecting two patterns. Known scripts correlated highly with each other and showed no correlation with the Braille-control pair. No correlation between neural RDMs and the model emerges. **(D)** Cross-script decoding. The mean of cross-decoding across all pairs of linguistic conditions showed significant above-chance decoding, hinting at generalization effects. Different individual pairs can be decoded from one script to another, while RW-PW shows an almost-significant trend (p = 0.052). IN all the figures, stars represent statistical significance (* p ≤ 0.05, ** p ≤ 0.01, *** p ≤ 0.001). Error bars represent standard error.

Discussion

We investigated the neural basis of processing a peculiar script, visual Braille, that differs from most common scripts (Changizi et al., 2006) for its lack of apparent shape features. We found, in expert readers, a preference for words written in Braille over scrambled arrangements of dots in the visual word form area, as well as multivariate neural representations of linguistic

content similar to the one of the participants' native script. Despite these similarities, we did not find generalization of the neural representation between scripts. We found similar multivariate processing of written text beyond VWFA, in the early stages of visual processing (V1), in shape-sensitive areas (LO), and in higher-order linguistic ones (l-PosTemp), where we also observe successful generalization of the two scripts and thus a script-invariant representation of linguistic properties.

Several studies showed increased selectivity in VWFA emerging with the acquisition of reading abilities (Dehaene et al., 2015; Dehaene-Lambertz et al., 2018). This sensitivity was investigated in the acquisition of specific scripts (e.g. Hebrew (Baker et al., 2007)) and in the association of pictures of houses with phonemes (L. Martin et al., 2019), suggesting that VWFA could globally link symbols with their represented linguistic properties acquired through learning. Other studies emphasized the importance of shape features for the location and activation of VWFA (Dehaene et al., 2005). However, none of these studies elucidates whether shape (global form extracted from joined lines) is a mandatory feature to activate VWFA (Ben-Shachar et al., 2007; Roberts et al., 2013; Vogel et al., 2012; Xue & Poldrack, 2007). Visual Braille, and its absence of explicit shapes, directly tests the impact of this visual feature common to scripts. We observed that VWFA, defined through Latin script, at the whole-region level responded strongly to Braille in the expert group, significantly more than randomly scattered dots. The selectivity we observe is limited to expert visual readers of Braille and not present in participants naïve to Braille. These findings show reorganization in the experts' brains as a consequence of their training and experience in reading visual Braille. Despite the deep differences in visual characteristics, reading visual Braille activates similar brain regions as other typical scripts do. These results suggest that the impact visual features have on VWFA is smaller than the symbolic meaning of the stimuli. In this regard, our study is supported by works on connectivity (Saygin et al., 2016; Op de Beeck et al., 2019; Wang et al., 2022), showing interactions between the (prospect) site of VWFA and language processing, further demonstrating its role as a connector between different areas and networks. For instance, previous work has shown that le location of what will become the VWFA after learning to read, can be predicted from structural and functional connectivity recorded in infants before they learn to read (Saygin et al., 2016).

Through a series of multivariate analyses, we demonstrated that the coding principles for linguistic material are similar between scripts known by the groups of participants. Differences between patterns emerged based on the expertise of a script rather than its visual features. In other words, when the visual Braille is known, it is represented similarly to the native, line-based alphabet. When we consider the patterns of brain activity elicited by our various

linguistic conditions, a clear and graded multivoxel selectivity appears evident for visual Braille for conditions with a different lexical status and orthographic properties: Real Words, Pseudo-Words, Non-Words (consonant strings), and scrambled dot patterns. This selectivity was virtually absent in naive participants reading Braille. Furthermore, the coding principles for Braille appeared strikingly similar and strongly correlated to those relative to the Latin-based script.

Whereas visual Braille processing is characterized by similar activations and coding principles compared to a shape-based script, an absence of cross-script generalization demonstrates that the representations of linguistic properties in VWFA remain intertwined with the specific visual properties of a script. There is no invariance for script. These results are in line with previous observations of similar coding principles for linguistic properties implemented within different sub-populations of VWFA for separate scripts (Lerma-Usabiaga et al., 2018; Yeatman & White, 2021; Zhan et al., 2023). In bilinguals, high similarity was present in activated neural populations between French and English, but less so between French and Chinese (Zhan et al., 2023). However, bilinguals might activate sounds with the two scripts. In our study, we can disentangle language and visual form. The Latin-based script and visual Braille are visually highly dissimilar, but they both map onto the same French words and the same sounds. If the activity patterns in VWFA would partially reflect phonological processes, or if there would be any other cascading effect from one script to the other, then we should have found significant cross-decoding.

Other visual areas showed mixed evidence regarding a preference for visual Braille compared to scrambled dots. First, we observed no univariate differences between Braille and Scrambled Braille in V1 and shape-selective LO. However, these regions showed similar multivariate profiles to the one identified in VWFA. Similar patterns of linguistic distance between known scripts reveal a widespread expertise-induced plasticity of selectivity in the visual system. Although studies of visual word forms focused mainly on VWFA, more widespread linguistic selectivity have been observed for shape-based scripts across the occipito-temporal cortices (Szwed et al., 2014; Siuda-Krzywicka et al., 2016). Although V1 has already been associated with broader plasticity effects and preference for particular scripts (e.g. Latin-based and Chinese (Szwed et al., 2014)), it is remarkable that such adaptation extends to a script that lacks explicit shape cues. Similarly, it is striking that LO shows significant coding of word-like stimuli. Previous studies on the gradient of involvement in word processing (Vinckier et al., 2007) did not perform such multivariate analyses, so possibly the literature underestimates the involvement of LO in word processing. Most relevant for our current purposes, the multivariate profile in LO is not a simple consequence of visual

differences, as this representation was not observed in controls for Braille, nor is it restricted to typical script shape processing, as we also observed this coding in visual Braille for experts.

In the language network, we reliably identified activated voxels in the left posterior temporal area (l-PosTemp) with limited preference for visual Braille over scrambled dots, but with significant decoding of the different conditions. Here, different classifications for orthographic and non-orthographic stimuli are to be expected, both in the canonical Latin-based and Braille script, as there is no doubt that individuals who read Braille interpret the dot patterns and reach the same level of comprehension. Although the neural patterns for known scripts presented strong correlations with each other, we found no correlation with the linguistic distance model. The lack of correlations may be attributed to the model, inspired by results shown in vOTC (Vinckier et al., 2007), a region highly sensible to visual input. It is possible that the role in phonological processing (Bhaya-Grossman & Chang, 2022; Chang et al., 2010) and reading (A. Martin et al., 2015) influences the relationships between linguistic properties in a non-linear manner. The preferential processing of phonological content could lead to more similarity between words and Pseudo-Words, and more dissimilar to low frequency phonological categories (Non-Words and Fake Script). The generalization across scripts suggests representations of linguistic conditions that is invariant to the visual differences. Such common script-invariant representation further demonstrates that at this stage, linguistic information is abstracted from the visual properties of the stimuli processed in the ventral occipito-temporal cortex (A. Martin et al., 2015).

Lastly, we acknowledge that due to the rarity of visual Braille expertise concomitant with availability and compatibility with MRI experimentation, we could only include six visual Braille experts. Nevertheless, our mean effect sizes across regions and main effects are large (mean D = 1.8, mean $\eta^2_p = 0.25$) and effects are very consistent among experts for both experiments (figures 2 and 3), which allow for strong conclusions (Smith & Little, 2018). With a restricted sample size, searching for expertise-related individual differences is not feasible. If anything, we can derive from the high consistency among experts that such interindividual differences might be small. We overcame the sample limitations through two different approaches. To help come to robust comparisons with non-experts, we included a control group twice as large as the experts in the study. For maximal sensitivity, we designed our experiment based on precision neuroimaging (Saxe et al., 2006) where each functional region of interest is localized in individual participants (Fedorenko et al., 2010).

Overall, we found major and widespread effects of expertise in visual Braille. Despite the major differences in the visual properties of Braille and Latin-based scripts, the regions showing a

preference for visual Braille in experts and the coding principles followed are remarkably similar to what we find for a Latin-based script. Yet, the neuronal populations that implement these principles do not overlap, demonstrating a strong effect of visual properties at a distributed activity level.

Methods

Participants

A total of twenty-three participants took part in the data acquisition. Data from five subjects were discarded due to incomplete acquisitions (three subjects) or inability to functionally localize VWFA for the Latin-based script (two subjects), resulting in eighteen subjects in the final sample. Six of them (6 females, mean age = 38.2 ± 11.4) were experts in reading Braille visually and twelve (10 females, mean age = 39.3 ± 10.4) were controls naïve to Braille alphabet. To determine visual Braille expertise, we asked expert participants to report their use of visual Braille as a declarative number of years spent working with / using Braille (mean expertise = 5.25 ± 5.43 years) and we assessed their reading speed through a behavioural reading test. All expert readers were presented with the same list of 30 words and instructed to read as many words as possible out loud in the given time of 1 minute (mean number of words read = 12.2 ± 6.11 words; range = 6-23).

Functional localization experiment

We designed a functional localizer to define VWFA, selective for words, and bilateral Lateral Occipital area (LO), selective for object's shape. We included six conditions of stimuli (Figure 1A): concrete French words expressed in the Latin alphabet (FW), the same French words presented in the Braille alphabet (BW), line drawings of the objects represented by the words (LD), and scrambled conditions for each of the 'intact' categories (scrambled Latin words, SFW; scrambled Braille words, SBW; scrambled line drawings, SLD). We selected 20 items for each condition. Latin words were selected from the Lexique 3.83 (New et al., 2005) and comprised of a length between 4 and 8 letters, and a frequency between 1 and 20 appearances per million words. Braille script words were the literal transcription of the Latin-based script words (*Code Braille Français Uniformisé Pour La Transcription Des Textes Imprimés (CBFU) Réalisé*, 2008). Line drawings came from two images datasets (Brodeur et al., 2010; Rossion & Pourtois, 2004). If necessary, we manipulated the colour information by obtaining grayscale stimuli that presented only the essential lines of the drawings. Scrambled conditions were created through two different custom algorithms, applied to each 'intact'

stimulus. Scrambling of Latin words and line drawings were the result of the re-arrangement of different parts of the corresponding 'intact' stimulus image in a grid-like manner. The scrambled Braille condition was created by randomizing the position of dots of each 'intact' Braille word. Different scrambling methods to ensure the alteration of each word's visual properties, line junctions in the case of Latin words and organization of dots in the case of Braille words. The localizer experiment included two block-design runs. In each run, participants were presented with 6 blocks of 10 stimuli presented for 1 second in white on a black background (Inter Stimulus Interval, ISI = 0.1s; Inter Block Interval, IBI = 6s). The order of the blocks was randomized, while ensuring that one condition was not presented in two consecutive blocks and that the first three blocks of a run were also presented at the end of the same run, in reverse order. Participants performed a 1-back task with a button press and were asked to detect an immediate repetition of the same stimulus (10% of the trials, so once per block). All stimuli subtended a frame of 520 x 208 pixels, corresponding to 6.1 and 2.5 degrees of visual angle in the MRI scanner, respectively.

Linguistic organization experiment

Inspired by Vinckier and colleagues (Vinckier et al., 2007), we designed four different conditions in a linguistic gradient fashion (figure 1B). (1) Real Words (RW) possessed semantic, phonological, and orthographical properties. This set was composed of French words (New et al., 2005) six letters length, with high frequency (>1 per million), and high identifiability (definition of lemma > 90%). Additionally, we controlled bigram and trigram frequency (top 45th percentile (Gimenes et al., 2020)). (2) Pseudo-Words (PW) were based on Real Words by identifying stimuli from the French Lexicon Project (Ferrand et al., 2010). We ensured bi- and tri-grams composing Pseudo-Words to have the same frequency of the real word set. Additionally, we measured Levensthein distance (the number of additions, deletions, transformations necessary to transform one string into another) and only included elements with a distance of 2, to avoid excessive similarity and possible confusion with the subset of Real Words. The final set of stimuli possesses both orthographic and phonological regularities similar to Real Words, but without semantic meaning. (3) For Non-Words (NW), we selected strings of consonants based on infrequent bigrams and trigrams (Gimenes et al., 2020), to create phonological distance between sets. We created the Braille conditions for all these categories by transliteration of the Latin conditions. (4) Fake Script (FS). For the Latin Fake Script, we transliterated the Non-Words set to a custom-made alphabet that maintained the same features of the original consonants, but in re-arranged line junctions. For Braille Fake Script, given the lack of evident shapes to re-arrange, we scrambled the dots arrangement as for the functional localizer. For each condition, we selected twelve six-characters long different stimuli. This composition of stimuli, comparable with the one made by Vinckier and colleagues

(Vinckier et al., 2007), created a linguistic gradient of words with meaning, phonology, and orthography, progressively stripped one of those properties. The experiment was divided into twelve runs of blocked design, alternating between runs with Latin and with Braille stimuli (Figure 1B). Participants performed a 1-back task, reacting to stimuli repetitions (targets). The presentation of stimuli within a block and run was pseudo-randomized to balance the appearance of targets across runs, categories, and position of the stimulus repeated. A total of six targets in each run were presented (12.5% of all stimuli). We controlled for the order of blocks and, within a block, for the order of categories and single stimuli. All parameters were balanced, resulting in a fixed experiment design which participants performed almost in the same order, aside from the counter-balanced alternation of the starting script, either Latin or Braille. During each block, four stimuli were presented in white on a black background for 3.5s (ISI jittered = 0.8s, 1s, 1.2s; IBI = 6s), each block lasting ~ 17-21.5s including target. The long stimulus presentation time is based on results from a previous study on experts' habituation to Braille words (Coquillart et al., 2022). All stimuli subtended a frame of 500 x 200 pixels, corresponding to 5.9 and 2.4 degrees of visual angle in the MRI scanner, respectively.

fMRI acquisition and pre-processing

This method section was automatically generated using bidspm (Gau et al., 2022). Fourteen participants completed the experiment in the expected single-session acquisition. Due to time constraints with the fMRI schedule or technical issues, four subjects took part in an additional session to conclude the full data acquisition. We tested all the participants using a 3T GE (Signa™ Premier, General Electric Company, USA, serial number: 000000210036MR03, software: 28\LX\MR, Software release: RX28.0_R04_2020.b) MRI scanner with a 48-channel head coil at the University Hospital of St Luc, Belgium. We acquired a whole-brain T1-weighted anatomical scan (3D-MPRAGE; 1.0 x 1.0 mm in-plane resolution; slice thickness 1mm; no gap; inversion time = 900 ms; repetition time (TR) = 2189,12 ms; echo time (TE) = 2.96 ms; flip angle (FA) = 8°; 156 slices; field of view (FOV) = 256 x 256 mm2; matrix size= 256 X 256). All functional runs were T2*-weighted scans acquired with Echo Planar and gradient recalled (EP/GR) imaging (2.6 x 2.6 mm in-plane resolution; slice thickness = 2.6mm; no gap; Multiband factor = 2; TR = 1750ms, TE = 30ms, 58 interleaved ascending slices; FA = 75°; FOV = 220 x 220 mm2; matrix size = 84 X 84). We extracted NIfTI files using MRIcroGL (https://github.com/rordenlab/MRIcroGL) and converted the content in BIDS format (Gorgolewski et al., 2016). We pre-processed the (f)MRI acquisitions with bidspm (Gau et al., 2022) (v3.1.0dev) using statistical parametric mapping SPM12 (version 7771) using MATLAB (R2021b) on a macOS computer (13.0.1). The pre-processing consisted of slice timing correction, realignment and unwarping, segmentation and skull-stripping, normalization to the Montreal Neuroimaging Institute (MNI) standard space, smoothing. Slice timing correction

used the 28th slice as a reference (interpolation: sinc interpolation). Functional scans were realigned and unwarped using the mean image as a reference (SPM single pass with 6 degrees of freedom). The anatomical image was corrected for bias and segmented using a unified segmentation. The mean functional image from realignment was co-registered to the bias-corrected anatomical image (degrees of freedom: 6). The transformation matrix from this co-registration was applied to all the functional images. The deformation field was applied to all the functional images (target space: IXI549Space; interpolation: 4th-degree b-spline). Finally, we applied spatial smoothing using a 3D Gaussian kernel (functional localizer, FWHM = 6 mm; main experiment, FWHM = 2mm). These smoothed, normalised BOLD images served as inputs to statistical analyses.

Generalised Linear Models (GLMs)

For both experiments, we analysed fMRI acquisitions with bidspm (v3.1.0dev) and SPM12 (version 7771) using the same MATLAB (R2021b) on a macOS computer (13.0.1). For the localizer experiment, at the subject level, we performed a univariate analysis with a linear regression at each voxel of the brain, using generalized least squares with a global FAST model and a high-pass filter (278 seconds cut-off). Image intensity scaling was done run-wide before statistical modelling such that the mean image would have a mean intracerebral intensity of 100. Block timings were convolved with SPM canonical hemodynamic response function (HRF) for the 6 stimuli categories (intact and scrambled Latin words, Braille words, Line drawings), in addition to ‘response’ and ‘target’ events of no interest and 6 head motion parameters (three translations, on the X, Y, Z axes, and three rotations) to account for motion artefacts. We computed four main contrasts: intact over scrambled Latin words (FW > SFW), Braille words over scrambled dots (BW > SBW), intact over scrambled line drawings (LD > SLD), intact and scrambled Latin words over rest (FW+SFW > rest). We used the [FW > SFW] and [BW > SBW] contrasts to independently localize VWFA in all the subjects, for Latin and for Braille. We tested the statistical significance of clusters identified in the [BW > SBW] contrast in or near the Latin-based VWFA, by applying Small Volume Correction (SVC) within a 10mm radius from the peak coordinates extracted from [FW > SFW]. We investigated the overlap between the two localizations of VWFA, by computing Dice coefficients. From masks of the two contrasts ($p_{uncorr} = 0.001$), we calculated the overlap as the intersection of the masks divided by the sum of total voxels in the identified areas. We localized bilaterally the Lateral Occipital area (LO) by the [LD > SLD] contrast. Lastly, we localized V1 by the [FW+SFW > rest] contrast. In the main experiment GLM, we included 8 regressors of interest for stimuli conditions (Real Words, Pseudo-Words, Non-Words, Fake Script for both Latin and Braille

scripts), and 8 regressors of no-interest (1 for targets; 1 for responses; 6 for head motion parameters). Contrast images were spatially smoothed using a 3D Gaussian kernel (FWHM = 2). The results of the main GLM were concatenated into 4D maps, to be included in the multivariate pattern analyses.

Eye-movements control analysis

To exclude potential confounds of eye movements, we computed eye displacement and integrated it in a Generalised Linear Model (GLM) as a regressor of no interest. We used bidsMReye (Gau & Cabee, 2023), a BIDS app relying on deepMReye (Frey et al., 2021) to decode eye motion from fMRI time series data, in particular from the MR signal of the eyeballs. Each run, the following values were computed: variance for the X gaze position, variance for the Y gaze position, framewise gaze displacement, number of X gaze position outliers, number of Y gaze position outliers, and number of gaze displacement outliers. Outliers were robustly estimated using an implementation of the median rule (Carling, 2000). We then used the newly assessed parameters to perform two additional subject-level GLM analyses. We added the eye displacement for each run to the regressors of no interest, and computed the same contrasts of the localizer GLM analysis. This analysis did not reveal significant activations in the investigated areas due to eye movements (figure S2). Therefore, the definition of the regions of interest described in the next section refers to the GLM described at the beginning of the section “Generalised Linear Model”.

Definition of the regions of Interest (ROIs)

To investigate the gradient of linguistic representations across low-level sensory and higher-order associative brain regions we defined multiple ROIs, namely: V1, LO, VWFA and left Posterior Temporal cortex (PosTemp), using intersections between neuroanatomy, existing literature and brain activation from our functional localizer. For VWFA, we first identified the peak activation in the activation map of the [FW > SFW] contrast within a 10mm sphere around the canonical coordinates (Cohen et al., 2000) of VWFA ([-45, -56, -16]) in each subject. We then expanded a progressively larger sphere from the individual peak coordinates and intersected this sphere with the activation map of the same [FW > SFW] contrast until the ROI comprised 100 voxels. Next, we overlapped the resulting mask with the functional mask downloaded from the neurosynth database (Yarkoni et al., 2011) (term: “visual words”) to control for expansions in unrelated regions. We used a similar process to localize bilateral LO from the [LD > SLD] contrast. We started from peak coordinates (Left LO: [-47, -70, -5], right LO: [47, -70, -5]) and applied a 10mm sphere around each set of coordinates to identify individual peaks in the localized [LD > SLD] activation. We then expanded a sphere from the individual peaks until a minimum threshold of 100 voxels was reached. Lastly, we overlapped

the expansion with the neurosynth mask for the term “object”. To identify early visual cortex (V1), we overlapped the bilateral brain mask from the Anatomy toolbox (Eickhoff et al., 2005) for bilateral V1 with a [FW + SFW > rest] contrast. For subsequent analyses on areas of the language network, we relied on parcels from Fedorenko and colleagues(Fedorenko et al., 2010). For each subject, we overlapped activations for the [FW > SFW] contrast to the different language parcels to identify brain regions that consistently responded to linguistic stimuli across subjects. Through this process, we highlighted left Posterior Temporal (l-PosTemp) activation in the majority (15 out of 18) of our participants. As this was the only area present in more than 80% of the participants, we chose it as the focus of our analysis.

Multivariate Pattern Analyses

To test the gradient of linguistic representations we performed multivariate pattern analyses using the CoSMoMVPA toolbox (Oosterhof et al., 2016) combined with custom MATLAB code (version 2021b). We applied this method to all the regions described in the section “ROI definition”. To obtain decoding accuracies, we performed feature selection across individuals by restricting the number of features to correspond to the number of voxels in the smallest ROI extracted through each method. This resulted in the feature selection of 43 voxels for LO and VWFA, extracted through the functional localizers, 62 for l-PosTemp, and 81 for V1. We then trained a support vector machine (‘libsvm’) in a leave-one-run-out fashion. To identify an organization of linguistic content, we performed pair-wise decoding, obtaining six comparisons per script (RW-PW, RW-NW, RW-FS, PW-NW, PW-FS, NW-FS). To compare the representational patterns emerging from the pairwise decoding accuracies, we performed Representational Similarity Analysis (Kriegeskorte et al., 2008) (RSA). We created a Representational Dissimilarity Matrix (RDM) for each group and script, where the value in each cell is given by the binary decoding accuracy of the classifier for that comparison. Resulting RDMs represent the linguistic (dis)similarity between stimulus conditions. Additionally, we correlated each neural RDM to a model of linguistic distance based on the number of features shared by each stimulus category. To build this matrix, we assigned a value to the corresponding number of linguistic properties (i.e. 3 to Real Words, 2 to Pseudo-Words, 1 to Non-Words, 0 to Fake Script) and then divided by the maximum value to obtain a scale from 0 to 1. We performed the correlations between neural matrices by applying non-parametrical statistical tests (Stelzer et al., 2013; Mattioni et al., 2020). When comparing two conditions, we first computed the correlation for each individual of the first condition to the group average of the second condition. For conditions from the same group (e.g. experts-Latin and experts-Braille), we averaged the group RDM of the second condition by excluding the subject being compared. We then averaged the individual correlations. Next, we performed the same correlation in the other direction, correlating each individual RDM from the second condition

to the first condition averaged (with the same precaution), and then calculated the mean of these correlations. We then averaged the correlations obtained from the two directions, obtaining the correlation between the two matrices. Lastly, to assess the generalizability of the decoding from one script to the other, we performed cross-script decoding. We limited our analyses to visual Braille experts, the only group showing significant decoding for both scripts in our ROIs. For each script, we trained our multi-voxel classifier on pair-wise linguistic differences within a script and tested the classification on the other script. We performed this classification reversely for both alphabets and averaged across the two directions.

Statistical analyses

Given the inter-subject variability in the localization of functional regions, all our analyses were carried out in individually localized ROIs (see ROI definition). To test between groups differences in VWFA activation for the [BW > SBW] contrast, we applied a Chi-square test on the number of participants who showed activation for such contrast. Additionally, we performed Pearson's' correlation between the words-per-minute reading speed of the expert visual Braille readers and their peak VWFA activation for the [BW > SBW] contrast. To test statistical significance of overall decoding accuracies we performed one-tail t-tests against chance level (mu = 0.5). To test group-script differences, we performed two-tailed t-tests with other script-group pairs to test for significant differences in the decoding accuracy. If the pairs referred to the same group (e.g. Latin, experts and Braille, experts), we performed paired t-tests. In all the t-tests, we additionally calculated Cohen's D effect size measure. We applied repeated measures ANOVA (6 stimuli conditions * 2 groups) to test for pairwise decoding accuracy differences between groups, within each script and each ROI. Effect size was estimated through partial eta-squared (η^2_p) measures. Effect sizes for bilateral LO, V1, and pSTS, can be found in Supplementary Material, in tables S3-S5-S7-S9. Additionally, we applied post-hoc t-tests to assess which conditions drove the effect of conditions. Correlations between RDMs were tested through non-parametric statistics. For each correlation between neural matrices, we constructed a null distribution by creating 10000 matrices with shuffled labels and calculating the corresponding correlations. We shuffled both correlation directions and then averaged the distributions for each direction separately and then between directions. The result was a null distribution of 10000 values representing correlations between conditions with shuffled labels. We then compared the correlations obtained from the matrices with intact labels to said distribution and extract a measure of the significance. In the case of correlations between neural-RDMs and our linguistic distance model, we only shuffled labels regarding each subject of one group and the model itself. The final result was again a null distribution of 10000 values representing correlations between conditions with shuffled labels. We then

applied the same steps to obtain p-values relative to each observed correlation. The p values in the rmANOVA post-hoc t-test were corrected using Bonferroni correction. All p values in the MVPA analyses were corrected for multiple comparisons with false discovery rate (FDR) corrections.

References

Baker, C. I., Liu, J., Wald, L. L., Kwong, K. K., Benner, T., & Kanwisher, N. (2007). Visual word processing and experiential origins of functional selectivity in human extrastriate cortex. *Proceedings of the National Academy of Sciences*, *104*(21), 9087–9092. https://doi.org/10.1073/pnas.0703300104

Ben-Shachar, M., Dougherty, R. F., Deutsch, G. K., & Wandell, B. A. (2007). Differential Sensitivity to Words and Shapes in Ventral Occipito-Temporal Cortex. *Cerebral Cortex*, *17*(7), 1604–1611. https://doi.org/10.1093/cercor/bhl071

Bhaya-Grossman, I., & Chang, E. F. (2022). Speech Computations of the Human Superior Temporal Gyrus. *Annual Review of Psychology*, *73*(1), 79–102. https://doi.org/10.1146/annurev-psych-022321-035256

Biederman, I. (1987). *Recognition-by-Components: A Theory of Human Image Understanding*.

Bola, Ł., Radziun, D., Siuda-Krzywicka, K., Sowa, J. E., Paplińska, M., Sumera, E., & Szwed, M. (2017). Universal Visual Features Might Be Necessary for Fluent Reading. A Longitudinal Study of Visual Reading in Braille and Cyrillic Alphabets. *Frontiers in Psychology*, *8*. https://doi.org/10.3389/fpsyg.2017.00514

Bramão, I., Reis, A., Petersson, K. M., & Faísca, L. (2011). The role of color information on object recognition: A review and meta-analysis. *Acta Psychologica*, *138*(1), 244–253. https://doi.org/10.1016/j.actpsy.2011.06.010

Brodeur, M. B., Dionne-Dostie, E., Montreuil, T., & Lepage, M. (2010). The Bank of Standardized Stimuli (BOSS), a New Set of 480 Normative Photos of Objects to Be

Used as Visual Stimuli in Cognitive Research. *PLoS ONE*, *5*(5), e10773. https://doi.org/10.1371/journal.pone.0010773

Büchel, C., Price, C., & Friston, K. (1998). A multimodal language region in the ventral visual pathway. *Nature*, *394*(6690), 274–277. https://doi.org/10.1038/28389

Carling, K. (2000). Resistant outlier rules and the non-Gaussian case. *Computational Statistics & Data Analysis*, *33*(3), 249–258. https://doi.org/10.1016/S0167-9473(99)00057-2

Chang, E. F., Rieger, J. W., Johnson, K., Berger, M. S., Barbaro, N. M., & Knight, R. T. (2010). Categorical speech representation in human superior temporal gyrus. *Nature Neuroscience*, *13*(11), 1428–1432. https://doi.org/10.1038/nn.2641

Changizi, M. A., Zhang, Q., Ye, H., & Shimojo, S. (2006). *The Structures of Letters and Symbols throughout Human History Are Selected to Match Those Found in Objects in Natural Scenes.* 23.

Code braille français uniformisé pour la transcription des textes imprimés (CBFU) Réalisé. (2008). *76*(3), 61–64.

Cohen, L., Dehaene, S., Naccache, L., Lehéricy, S., Dehaene-Lambertz, G., Hénaff, M.-A., & Michel, F. (2000). The visual word form area: Spatial and temporal characterization of an initial stage of reading in normal subjects and posterior split-brain patients. *Brain: A Journal of Neurology*, *123*, 291–307.

Cohen, L., Lehéricy, S., Chochon, F., Lemer, C., Rivaud, S., & Dehaene, S. (2002). Language-specific tuning of visual cortex? Functional properties of the Visual Word Form Area. *Brain*, *125*(5), 1054–1069. https://doi.org/10.1093/brain/awf094

Coquillart, N., Collignon, O., Cerpelloni, F., & Van Audenhaege, A. (2022). *Lecture visuelle du braille et plasticité cérébrale. Zoom sur l'aire visuelle de la forme des mots* [UCLouvain]. https://dial.uclouvain.be/memoire/ucl/object/thesis:37423

Definition of shape. (n.d.). https://dictionary.cambridge.org/dictionary/english/shape

Dehaene, S., & Cohen, L. (2011). The unique role of the visual word form area in reading. *Trends in Cognitive Sciences*, *15*(6), 254–262. https://doi.org/10.1016/j.tics.2011.04.003

Dehaene, S., Cohen, L., Morais, J., & Kolinsky, R. (2015). Illiterate to literate: Behavioural and cerebral changes induced by reading acquisition. *Nature Reviews Neuroscience*, *16*(4), 234–244. https://doi.org/10.1038/nrn3924

Dehaene, S., Cohen, L., Sigman, M., & Vinckier, F. (2005). The neural code for written words: A proposal. *Trends in Cognitive Sciences*, *9*(7), 335–341. https://doi.org/10.1016/j.tics.2005.05.004

Dehaene, S., Pegado, F., Braga, L. W., Ventura, P., Filho, G. N., Jobert, A., Dehaene-Lambertz, G., Kolinsky, R., Morais, J., & Cohen, L. (2010). How Learning to Read Changes the Cortical Networks for Vision and Language. *Science*, *330*(6009), 1359–1364. https://doi.org/10.1126/science.1194140

Dehaene-Lambertz, G., Monzalvo, K., & Dehaene, S. (2018). The emergence of the visual word form: Longitudinal evolution of category-specific ventral visual areas during reading acquisition. *PLOS Biology*, *16*(3), e2004103. https://doi.org/10.1371/journal.pbio.2004103

Eickhoff, S. B., Stephan, K. E., Mohlberg, H., Grefkes, C., Fink, G. R., Amunts, K., & Zilles, K. (2005). A new SPM toolbox for combining probabilistic cytoarchitectonic maps and functional imaging data. *NeuroImage*, *25*(4), 1325–1335. https://doi.org/10.1016/j.neuroimage.2004.12.034

Fedorenko, E., Hsieh, P.-J., Nieto-Castañón, A., Whitfield-Gabrieli, S., & Kanwisher, N. (2010). New Method for fMRI Investigations of Language: Defining ROIs Functionally in Individual Subjects. *Journal of Neurophysiology*, *104*(2), 1177–1194. https://doi.org/10.1152/jn.00032.2010

Ferrand, L., New, B., Brysbaert, M., Keuleers, E., Bonin, P., Méot, A., Augustinova, M., & Pallier, C. (2010). The French Lexicon Project: Lexical decision data for 38,840

French words and 38,840 pseudowords. *Behavior Research Methods*, *42*(2), 488–496. https://doi.org/10.3758/BRM.42.2.488

Frey, M., Nau, M., & Doeller, C. F. (2021). Magnetic resonance-based eye tracking using deep neural networks. *Nature Neuroscience*, *24*(12), 1772–1779. https://doi.org/10.1038/s41593-021-00947-w

Gau, R., Barilari, Marco, Battal, Ceren, Rezk, Mohamed, Collignon, Olivier, Gurtubay, Ane, Falagiarda, Federica, MacLean, Michèle, Cerpelloni, Filippo, Shahzad, Iqra, Nunes, Márcia, Caron-Guyon, Jeanne, Chouinard-Leclaire, Christine, Yang, Ying, & Mattioni, Stefania. (2022). *Bidspm* (2.3.0) [Computer software]. Zenodo. https://doi.org/10.5281/ZENODO.3554331

Gau, R., & Cabee, P. (2023). *bidsMReye* (0.3.0) [Computer software]. Zenodo. https://doi.org/10.5281/zenodo.7574501

Gimenes, M., Perret, C., & New, B. (2020). Lexique-Infra: Grapheme-phoneme, phoneme-grapheme regularity, consistency, and other sublexical statistics for 137,717 polysyllabic French words. *Behavior Research Methods*, *52*(6), 2480–2488. https://doi.org/10.3758/s13428-020-01396-2

Gorgolewski, K. J., Auer, T., Calhoun, V. D., Craddock, R. C., Das, S., Duff, E. P., Flandin, G., Ghosh, S. S., Glatard, T., Halchenko, Y. O., Handwerker, D. A., Hanke, M., Keator, D., Li, X., Michael, Z., Maumet, C., Nichols, B. N., Nichols, T. E., Pellman, J., … Poldrack, R. A. (2016). The brain imaging data structure, a format for organizing and describing outputs of neuroimaging experiments. *Scientific Data*, *3*(1), 160044. https://doi.org/10.1038/sdata.2016.44

Grill-Spector, K., & Malach, R. (2004). THE HUMAN VISUAL CORTEX. *Annual Review of Neuroscience*, *27*(1), 649–677. https://doi.org/10.1146/annurev.neuro.27.070203.144220

Kriegeskorte, N., Mur, M., & Bandettini, P. (2008). Representational similarity analysis—Connecting the branches of systems neuroscience. *Frontiers in Systems Neuroscience*, *2*(NOV), 1–28. https://doi.org/10.3389/neuro.06.004.2008

Krizhevsky, A., Sutskever, I., & Hinton, G. E. (2017). ImageNet classification with deep convolutional neural networks. *Communications of the ACM*, *60*(6), 84–90. https://doi.org/10.1145/3065386

Landau, B., Smith, L. B., & Jones, S. S. (1988). The importance of shape in early lexical learning. *Cognitive Development*, *3*(3), 299–321. https://doi.org/10.1016/0885-2014(88)90014-7

Lerma-Usabiaga, G., Carreiras, M., & Paz-Alonso, P. M. (2018). Converging evidence for functional and structural segregation within the left ventral occipitotemporal cortex in reading. *Proceedings of the National Academy of Sciences*, *115*(42). https://doi.org/10.1073/pnas.1803003115

Li, J., Hiersche, K. J., & Saygin, Z. M. (2024). Demystifying the Visual Word Form Area: Visual and Nonvisual Response Properties of Ventral Temporal Cortex with precision fMRI. *bioRxiv*. https://doi.org/10.1101/2023.06.15.544824

Li, J., Osher, D. E., Hansen, H. A., & Saygin, Z. M. (2020). Innate connectivity patterns drive the development of the visual word form area. *Scientific Reports*, *10*(1), 18039. https://doi.org/10.1038/s41598-020-75015-7

Logothetis, N. K., & Sheinberg, D. L. (1996). *Visual Object Recognition*.

Marr, D., & Hildreth, E. (1980). *Theory of edge detection*.

Martin, A., Schurz, M., Kronbichler, M., & Richlan, F. (2015). Reading in the brain of children and adults: A meta-analysis of 40 functional magnetic resonance imaging studies. *Human Brain Mapping*, *36*(5), 1963–1981. https://doi.org/10.1002/hbm.22749

Martin, L., Durisko, C., Moore, M. W., Coutanche, M. N., Chen, D., & Fiez, J. A. (2019). The VWFA Is the Home of Orthographic Learning When Houses Are Used as Letters. *Eneuro*, *6*(1), ENEURO.0425-17.2019. https://doi.org/10.1523/ENEURO.0425-17.2019

Mattioni, S., Rezk, M., Battal, C., Bottini, R., Cuculiza Mendoza, K. E., Oosterhof, N. N., & Collignon, O. (2020). Categorical representation from sound and sight in the ventral

occipito-temporal cortex of sighted and blind. *eLife*, *9*, e50732. https://doi.org/10.7554/eLife.50732

New, B., Pallier, C., Ferrand, L., & Matos, R. (2005). Manuel de Lexique 3. *Behavior Research Methods, Instruments, & Computers*, *36*(3), 516–524.

Oosterhof, N. N., Connolly, A. C., & Haxby, J. V. (2016). CoSMoMVPA: Multi-Modal Multivariate Pattern Analysis of Neuroimaging Data in Matlab/GNU Octave. *Frontiers in Neuroinformatics*, *10*. https://doi.org/10.3389/fninf.2016.00027

Op de Beeck, H. P., Pillet, I., & Ritchie, J. B. (2019). Factors Determining Where Category-Selective Areas Emerge in Visual Cortex. *Trends in Cognitive Sciences*, *23*(9), 784–797. https://doi.org/10.1016/j.tics.2019.06.006

Pattamadilok, C., Planton, S., & Bonnard, M. (2019). Spoken language coding neurons in the Visual Word Form Area: Evidence from a TMS adaptation paradigm. *NeuroImage*, *186*, 278–285. https://doi.org/10.1016/j.neuroimage.2018.11.014

Planton, S., Chanoine, V., Sein, J., Anton, J.-L., Nazarian, B., Pallier, C., & Pattamadilok, C. (2019). Top-down activation of the visuo-orthographic system during spoken sentence processing. *NeuroImage*, *202*, 116135. https://doi.org/10.1016/j.neuroimage.2019.116135

Planton, S., Wang, S., Bolger, D., Bonnard, M., & Pattamadilok, C. (2022). Effective connectivity of the left-ventral occipito-temporal cortex during visual word processing: Direct causal evidence from TMS-EEG co-registration. *Cortex*, *154*, 167–183. https://doi.org/10.1016/j.cortex.2022.06.004

Price, C. J., & Devlin, J. T. (2003). The myth of the visual word form area. *NeuroImage*, *19*(3), 473–481. https://doi.org/10.1016/S1053-8119(03)00084-3

Price, C. J., & Devlin, J. T. (2004). The pro and cons of labelling a left occipitotemporal region: “The visual word form area”. *NeuroImage*, *22*(1), 477–479. https://doi.org/10.1016/j.neuroimage.2004.01.018

Price, C. J., & Devlin, J. T. (2011). The Interactive Account of ventral occipitotemporal contributions to reading. *Trends in Cognitive Sciences*, *15*(6), 246–253. https://doi.org/10.1016/j.tics.2011.04.001

Rajalingham, R., Kar, K., Sanghavi, S., Dehaene, S., & DiCarlo, J. J. (2020). The inferior temporal cortex is a potential cortical precursor of orthographic processing in untrained monkeys. *Nature Communications*, *11*(1), 3886. https://doi.org/10.1038/s41467-020-17714-3

Riesenhuber, M., & Poggio, T. (1999). Hierarchical models of object recognition in cortex. *Nature Neuroscience*, *2*(11), 1019–1025. https://doi.org/10.1038/14819

Roberts, D. J., Woollams, A. M., Kim, E., Beeson, P. M., Rapcsak, S. Z., & Lambon Ralph, M. A. (2013). Efficient Visual Object and Word Recognition Relies on High Spatial Frequency Coding in the Left Posterior Fusiform Gyrus: Evidence from a Case-Series of Patients with Ventral Occipito-Temporal Cortex Damage. *Cerebral Cortex*, *23*(11), 2568–2580. https://doi.org/10.1093/cercor/bhs224

Rossion, B., & Pourtois, G. (2004). Revisiting Snodgrass and Vanderwart's Object Pictorial Set: The Role of Surface Detail in Basic-Level Object Recognition. *Perception*, *33*(2), 217–236. https://doi.org/10.1068/p5117

Saxe, R., Brett, M., & Kanwisher, N. (2006). Divide and conquer: A defense of functional localizers. *NeuroImage*, *30*(4), 1088–1096. https://doi.org/10.1016/j.neuroimage.2005.12.062

Saygin, Z. M., Osher, D. E., Norton, E. S., Youssoufian, D. A., Beach, S. D., Feather, J., Gaab, N., Gabrieli, J. D. E., & Kanwisher, N. (2016). Connectivity precedes function in the development of the visual word form area. *Nature Neuroscience*, *19*(9), 1250–1255. https://doi.org/10.1038/nn.4354

Siuda-Krzywicka, K., Bola, Ł., Paplińska, M., Sumera, E., Jednoróg, K., Marchewka, A., Śliwińska, M. W., Amedi, A., & Szwed, M. (2016). Massive cortical reorganization in sighted Braille readers. *eLife*, *5*, e10762. https://doi.org/10.7554/eLife.10762

Smith, P. L., & Little, D. R. (2018). Small is beautiful: In defense of the small-N design. *Psychonomic Bulletin & Review*, *25*(6), 2083–2101. https://doi.org/10.3758/s13423-018-1451-8

Stelzer, J., Chen, Y., & Turner, R. (2013). Statistical inference and multiple testing correction in classification-based multi-voxel pattern analysis (MVPA): Random permutations and cluster size control. *NeuroImage*, *65*, 69–82. https://doi.org/10.1016/j.neuroimage.2012.09.063

Stevens, W. D., Kravitz, D. J., Peng, C. S., Tessler, M. H., & Martin, A. (2017). Privileged Functional Connectivity between the Visual Word Form Area and the Language System. *The Journal of Neuroscience*, *37*(21), 5288–5297. https://doi.org/10.1523/JNEUROSCI.0138-17.2017

Szwed, M., Dehaene, S., Kleinschmidt, A., Eger, E., Valabrègue, R., Amadon, A., & Cohen, L. (2011). Specialization for written words over objects in the visual cortex. *NeuroImage*, *56*(1), 330–344. https://doi.org/10.1016/j.neuroimage.2011.01.073

Szwed, M., Qiao, E., Jobert, A., Dehaene, S., & Cohen, L. (2014). Effects of Literacy in Early Visual and Occipitotemporal Areas of Chinese and French Readers. *Journal of Cognitive Neuroscience*, *26*(3), 459–475. https://doi.org/10.1162/jocn_a_00499

Tarr, M. J., & Bulthoff, H. H. (1998). *Image-based object recognition in man, monkey and machine*.

Vinckier, F., Dehaene, S., Jobert, A., Dubus, J. P., Sigman, M., & Cohen, L. (2007). Hierarchical Coding of Letter Strings in the Ventral Stream: Dissecting the Inner Organization of the Visual Word-Form System. *Neuron*, *55*(1), 143–156. https://doi.org/10.1016/j.neuron.2007.05.031

Vogel, A. C., Petersen, S. E., & Schlaggar, B. L. (2012). The Left Occipitotemporal Cortex Does Not Show Preferential Activity for Words. *Cerebral Cortex*, *22*(12), 2715–2732. https://doi.org/10.1093/cercor/bhr295

Wang, S., Planton, S., Chanoine, V., Sein, J., Anton, J.-L., Nazarian, B., Dubarry, A.-S., Pallier, C., & Pattamadilok, C. (2022). Graph theoretical analysis reveals the

functional role of the left ventral occipito-temporal cortex in speech processing. *Scientific Reports*, *12*(1), 20028. https://doi.org/10.1038/s41598-022-24056-1

Witzel, C., & Gegenfurtner, K. R. (2018). Color Perception: Objects, Constancy, and Categories. *Annual Review of Vision Science*, *4*(1), 475–499. https://doi.org/10.1146/annurev-vision-091517-034231

Xue, G., & Poldrack, R. A. (2007). The Neural Substrates of Visual Perceptual Learning of Words: Implications for the Visual Word Form Area Hypothesis. *Journal of Cognitive Neuroscience*, *19*(10), 1643–1655. https://doi.org/10.1162/jocn.2007.19.10.1643

Yarkoni, T., Poldrack, R. A., Nichols, T. E., Van Essen, D. C., & Wager, T. D. (2011). Large-scale automated synthesis of human functional neuroimaging data. *Nature Methods*, *8*(8), 665–670. https://doi.org/10.1038/nmeth.1635

Yeatman, J. D., & White, A. L. (2021). Reading: The Confluence of Vision and Language. *Annual Review of Vision Science*, *7*(1), 487–517. https://doi.org/10.1146/annurev-vision-093019-113509

Zhan, M., Pallier, C., Agrawal, A., Dehaene, S., & Cohen, L. (2023). Does the visual word form area split in bilingual readers? A millimeter-scale 7-T fMRI study. *Science Advances*.

Acknowledgements

The authors would like to thank the Institut Royal pour Sourds et Aveugles (IRSA) and the association EQLA for their help in recruiting the Braille experts. The project was funded in parts by a Mandat d'Impulsion Scientifique awarded to OC, the Belgian Excellence of Science (EOS) program (Project No. 30991544) awarded to HOB and OC, a Flagship ERA-NET grant SoundSight (FRS-FNRS PINT-MULTI R.8008.19) awarded to OC, and research project G0D3322N of the Fund for Scientific Research (FWO) Flanders and Methusalem project METH/24/003 awarded to HO. AV is a research fellow, CB and JM are postdoctoral researchers, and OC is a senior research associate at the Fond National de la Recherche Scientifique de Belgique (FRS-FNRS). FC received funding from a KU Leuven-UCLouvain cooperation grant.

Authors contributions

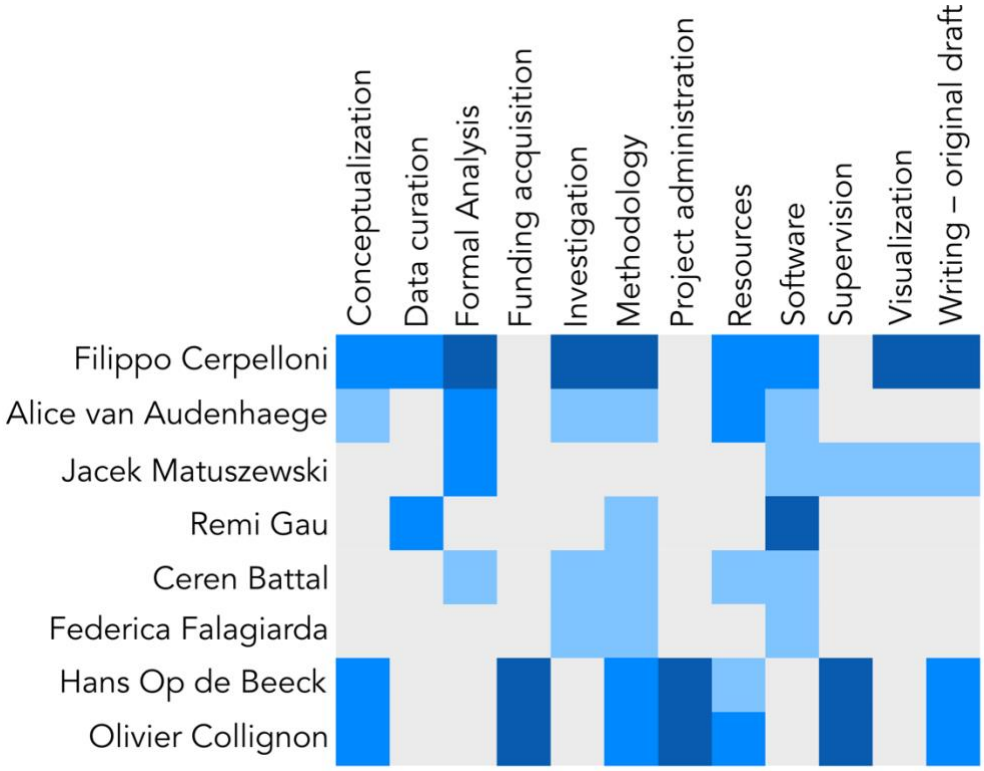

Figure 7 – Author contributions. Based on the CRedIT (https://credit.niso.org/) taxonomy. Each contribution was assessed as 'lead' (dark blue), 'equal' (mid blue), 'support' (light blue).